RESEARCH PAPER

Development of an anaesthetized-rat model of exercise hyperpnoea: an integrative model of respiratory control using an equilibrium diagram

Tadayoshi Miyamoto[1,2] (iD) | **Kou Manabe[1]** | **Shinya Ueda[1]** | **Hidehiro Nakahara[1]**

[1]Graduate School of Health Sciences, Morinomiya University of Medical Sciences, Osaka City, Osaka 559-0034, Japan

[2]Department of Cardiovascular Dynamics, National Cerebral and Cardiovascular Center Research Institute, Suita City, Osaka 565-8565, Japan

Correspondence
Tadayoshi Miyamoto, Graduate school of health sciences, Morinomiya University of Medical Sciences, 1-26-16 Nanko-Kita, Suminoe-Ku, Osaka City, Osaka 559-0034, Japan.
Email: miyamoto@morinomiya-u.ac.jp

Funding information
This study was supported in part by a Grant-in-Aid for Scientific Research (No. 15H03101) from the Japanese Ministry of Education, Culture, Sports, Science and Technology.

Edited by: Jeremy Ward

Abstract

Exercise-induced ventilatory abnormalities in various disease states seem to arise from pathological changes of respiratory regulation. Although experimental studies in small animals are essential to investigate the pathophysiological basis of various disease models, the lack of an integrated framework for quantitatively characterizing respiratory regulation during exercise prevents us from resolving these problems. The purpose of this study was to develop an anaesthetized-rat model for studying exercise hyperpnoea for quantitative characterization of the respiratory chemoreflex feedback system. In 24 anaesthetized rats, we induced muscle contraction by stimulating bilateral distal sciatic nerves at low and high voltage to mimic exercise. We recorded breath-by-breath respiratory gas analysis data and cardiorespiratory responses while running two protocols to characterize the controller and plant of the respiratory chemoreflex. The controller was characterized by determining the linear relationship between end-tidal CO_2 pressure (P_{ETCO_2}) and minute ventilation ($\dot{V}_E$), and the plant by the hyperbolic relationship between $\dot{V}_E$ and P_{ETCO_2}. During exercise, the controller curve shifted upward without change in controller gain, accompanying increased oxygen uptake. The hyperbolic plant curve shifted rightward and downward depending on exercise intensity as predicted by increased metabolism. Exercise intensity-dependent changes in operating points ($\dot{V}_E$ and P_{ETCO_2}) were estimated by integrating the controller and plant curves in a respiratory equilibrium diagram. In conclusion, we developed an anaesthetized-rat model for studying exercise hyperpnoea, using systems analysis for quantitative characterization of the respiratory system. This novel experimental model will be useful for understanding the mechanisms responsible for abnormal ventilatory responses to exercise in disease models.

KEYWORDS
animal models, chemoreflex, exercise, rat, respiratory control, ventilation

1 | INTRODUCTION

Exercise-induced ventilatory abnormalities in various disease states seem to arise from pathological changes in respiratory regulation (Arzt et al., 2003; Dempsey & Smith, 2014; Guazzi et al., 2007). Many experimental studies have attempted to determine the control mechanisms responsible for generating the ventilatory responses observed during exercise (Ainslie & Duffin, 2009; Dempsey, Miller, & Roman, 2006; Eldridge & Waldrop, 1991; Mateika & Duffin; 1995; Kao, 1963; Krogh & Lindhard., 1913; Wasserman, Whipp, & Casaburi, 1986). However intense debate remains over the major physiological mechanisms responsible for controlling ventilation during exercise (Dempsey & Smith, 2014; Forster, Haouzi, & Dempsey, 2012). Consequently, the pathophysiological mechanisms of abnormal ventilation during exercise under pathological conditions, such as congestive heart failure and chronic obstructive pulmonary disease, are also still unknown. Furthermore, the lack of useful small-animal models for investigating respiratory control during exercise makes it difficult to investigate the underlying mechanisms of exercise hyperpnoea and respiratory abnormalities.

The respiratory chemoreflex controlling ventilation is a negative feedback system that can be divided into two subsystems: a controller

New Findings

- **What is the central question of this study?**

  The lack of useful small-animal models for studying exercise hyperpnoea makes it difficult to investigate the underlying mechanisms of exercise-induced ventilatory abnormalities in various disease states.

- **What is the main finding and its importance?**

  We developed an anaesthetized-rat model for studying exercise hyperpnoea, using a respiratory equilibrium diagram for quantitative characterization of the respiratory chemoreflex feedback system. This experimental model will provide an opportunity to clarify the major determinant mechanisms of exercise hyperpnoea, and will be useful for understanding the mechanisms responsible for abnormal ventilatory responses to exercise in disease models.

(controlling element) and a plant (controlled element) (Figure 1; Berger, Mitchell, & Severinghaus, 1977; Defares, 1964; Folgering, 1988; Lloyd & Cunningham, 1963; Milhorn, 1966). Briefly, the controller element approximates a straight line and represents the linear increase in minute ventilation ($\dot{V}_E$; output) in response to an increase in arterial partial pressure of CO_2 (P_{aCO_2} input). The plant element approximates a hyperbola with a positive asymptote, and represents the asymptotic decrease of P_{aCO_2} (output) in response to an increase in $\dot{V}_E$ (input). Since respiration is determined from the intersecting point of the controller and the plant curves on the respiratory equilibrium diagram (Figure 1), quantitative analysis of the two subsystems of respiratory chemoreflex provides a framework by which we can analytically evaluate how the unique value of $\dot{V}_E$ during exercise is determined by the respiratory chemoreflex system, how changes in the controller element affect exercise hyperpnoea, and how changes in the plant element affect exercise hyper-

pnoea (Cummin & Saunders., 1987; Cunningham, Robbins, & Wolff, 1986). In human studies, we developed an experimental method for quantitative characterization of the respiratory control system at rest (Miyamoto et al., 2004, 2014, 2015) and during exercise (Miyamoto et al., 2012; Ogoh, Hayashi, Inagaki, Ainslie, & Miyamoto, 2008). Subsequently, we succeeded in characterizing these subsystems in an open-loop condition and constructed a respiratory equilibrium diagram to illustrate the mechanisms of respiratory regulation at rest in normal and CHF rats under anaesthesia (Miyamoto et al., 2006). However, there is no appropriate small-animal experimental model to investigate the exercise adaptation and/or pathophysiological key mechanisms responsible for controlling ventilation. The primary purpose of this study was to develop an anaesthetized-rat model for studying exercise hyperpnoea during electrically induced muscular contraction, using systems analysis for quantitative characterization of the respiratory chemoreflex feedback system.

2 | METHODS

2.1 | Ethical approval

All experimental procedures and protocols were performed in accordance with the *Guiding Principles for Care and Use of Animals in the Field of Physiological Sciences*, approved by the Physiological Society of Japan. Animals were housed on a 12 h–12 h light–dark cycle at 19–23°C and 55 ± 10% humidity and had *ad libitum* access to food and water. The experiments were approved by the Animal Subjects Committee of the Morinomiya University of Medical Sciences (No. 2014A005). Every attempt was made to reduce animal suffering and discomfort and to reduce the number of animals needed to obtain reliable results. All surgery was performed under general anaesthesia as described in the Experimental preparation section and no animals were reused for different protocols. At the end of the experiments, animals were killed by an overdose of sodium pentobarbitone (200 mg kg^{-1} i.v.).
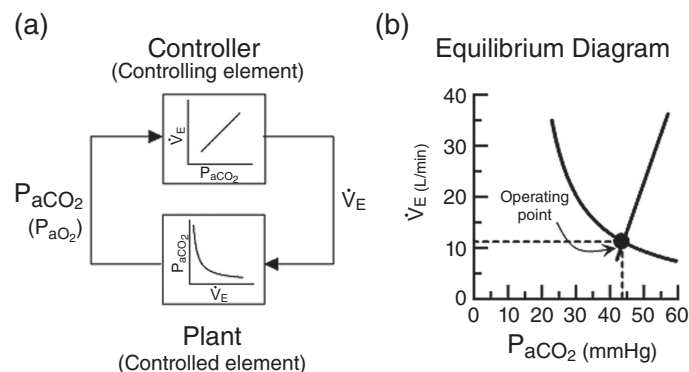

FIGURE 1 Block diagram of the respiratory chemoreflex feedback system and equilibrium diagram analysis characterizing the system. The respiratory chemoreflex system consists of two subsystems: the controller (controlling element) and the plant (controlled element). In the controller, the input parameter is P_{CO_2} and the output parameter is minute ventilation ($\dot{V}_E$). The controller can be characterized by observing changes in $\dot{V}_E$ in response to changes in arterial P_{CO_2} (P_{aCO_2}). In the plant, the input is $\dot{V}_E$ and the output is P_{aCO_2}. The plant can be characterized by observing changes in P_{aCO_2} in response to changes in $\dot{V}_E$ (a). Since both relationships share common variables, the resultant operating point of the ventilatory or P_{aCO_2} response under the closed loop condition is determined by the intersection of these two factors (b). P_{aO_2}, arterial P_{O_2}

2.2 | Experimental preparation

In two experimental protocols, 24 male Sprague–Dawley rats (body weight, 340–670 g) were used. Anaesthesia was initiated by an intraperitoneal bolus injection of a mixture of urethane (500 mg kg^{-1}; Sigma-Aldrich, St Louis, MO, USA) and α-chloralose (80 mg kg^{-1}; Sigma-Aldrich). The rats under anaesthesia were intubated and spontaneous breathing was preserved. The depth of anaesthesia was assessed by observing the presence or absence of a significant withdrawal reflex to pinching a paw and the absence of alterations in arterial blood pressure and heart rate. Throughout the experiment, a stable level of these variables was used as an indication of the anaesthetic level. All experimental protocols were completed within 3.5 h and supplemental dosing was not required during the experiment.

2.3 | Experimental set-up

Figure 2 shows the experimental set-up used for characterizing the respiratory chemoreflex feedback system in rats. The ventilatory responses were measured continuously using an open circuit apparatus. In protocol 1, 12 rats breathed through a tube attached to a low-resistance one-way valve. The electromagnetic valve mechanism attached to the inspiratory port allowed the rat to inspire room air or a selected gas mixture from a 40-litre Douglas bag containing CO_2 in O_2 with N_2 balance [fractional concentration of inspired CO_2 (F_{ICO_2}) = 0.00, 0.03 and 0.05; fractional concentration of inspired (F_{IO_2}) = 0.21 with N_2 balance]. The total apparatus dead space was 0.05 ml. In protocol 2, the other 12 rats breathed through a tube attached to small-animal ventilator (volume-controlled mechanical ventilator; model CIV-101, Columbus Instruments, Columbus, OH, USA). In both protocols, expired gas was sampled continuously, and O_2 and CO_2 concentrations were measured by a mass spectrometer (ARCO2000-MET, Arcosystem, Chiba, Japan). Expired gas flow was measured using a differential pressure transducer with sufficient sensitivity and frequency response, and a high precision soap-film flow meter (SF-1U/2U, Horiba Ltd, Kyoto, Japan). End-tidal CO_2 partial pressure (P_{ETCO_2}) was used as a surrogate for arterial partial pressure of CO_2 (P_{aCO_2}). Flow signals were converted to single breath data by matching to gas concentrations identified as single breaths using P_{ETCO_2}, after accounting for the time lag (950 ms) in gas concentration measurements. The corresponding O_2 uptake ($\dot{V}_{O_2}$) and CO_2 output ($\dot{V}_{CO_2}$) for each breath were calculated from the differences of inspired–expired gas concentrations and by expired ventilation, with inspired ventilation being calculated by N_2 correction. A catheter was placed in the right carotid artery and connected to a pressure transducer (BSM-7201, DX-200, Nihon Kohden, Tokyo, Japan) to measure arterial pressure. Heart rate was measured using a cardio-tachometer (AT601G, Nihon Kohden) triggered by the R-wave on the electrocardiogram. The heart rate series were checked by visual inspection. Body temperature was monitored with a thermometer placed in the rectum, and was maintained at 38°C using a heating pad throughout the experiment. Oxygen and CO_2 measurements were calibrated using a standard gas of known concentrations before each test. Signals from the mass spectrometer, flow sensor, pressure transducer and cardio-tachometer were synchronized on-line using a personal computer, and displayed continuously during all experiments. The signals were logged at 200 Hz using a 12-bit analog-to-digital converter (AD12-8(PM) CONTEC Co., Ltd, Osaka, Japan). The analytical software program was custom-made.

2.4 | Electrically induced muscle contraction mimicking exercise

Under the above experimental conditions, we simultaneously induced muscle contraction by stimulating bilateral distal sciatic nerves at low and high voltage (0.1–0.5 and 3.0 V, respectively) in the anaesthetized rat. Thus, the intensity of muscle contraction was controlled by varying the voltage (SEN-7130, Nihon Kohden) as shown in Figure 3. The stimulation electrodes and nerves were secured with silicone glue (Kwik- Sil, World, Precision Instruments, Sarasota, FL, USA). Electrically induced muscle contraction mimicking exercise was continued for 24 min using a stimulator. The muscles contracted rhythmically at stimulation frequency of 5 Hz (interval, 150 ms; duration, 2 ms) (Bassols, Carreras, & Cussó, 1986).

2.5 | Study design

2.5.1 | Methodological approaches to open feedback system in rats

The properties of a closed feedback system can be fully elucidated by examining its open-loop characteristics. One direct way is to open the loop physically. However, this approach is not always possible in a living body, because the exact location of CO_2 sensors is not known and the brain has to be isolated for that purpose. Therefore, we adopted a more practical approach. In previous small-animal studies (Bin-Jaliah, Maskell, & Kumar, 2005; Hayashi, Yoshida, Fukuda, & Honda, 1982), it is well known that arterial CO_2 tension can be manipulated easily by altering the inspiratory CO_2 tension, and $\dot{V}_E$ seems to have no effect on arterial CO_2 tension unless ventilation is greatly decreased. Based on this concept, we effectively opened the feedback loop and successfully examined the P_{aCO_2} to $\dot{V}_E$ relationship by changing the inspiratory CO_2 tension at rest and during muscle contraction. In humans, the $\dot{V}_E$ to P_{aCO_2} relationship can be obtained easily by voluntarily changing $\dot{V}_E$ to open the feedback loop (Miyamoto et al., 2004, 2012, 2014, 2015; Ogoh et al., 2008). The same method can be used in anaesthetized animals, using a mechanical ventilator.

2.5.2 | Assessment of respiratory equilibrium diagram

To characterize the respiratory chemoreflex system in normal rats, we divided the total system into two elements, the controller and plant (Figure 1a). The controller detects changes in P_{aCO_2} and alters $\dot{V}_E$ accordingly. Therefore, we can characterize the controller by observing changes in $\dot{V}_E$ in response to changes in P_{aCO_2}. The plant operates according to the command from the controller and expires carbon dioxide accordingly. As a result, P_{aCO_2} changes in response to changes in $\dot{V}_E$. Thus, the plant can be characterized by observing changes in P_{aCO_2} in response to changes in $\dot{V}_E$. The characteristics of
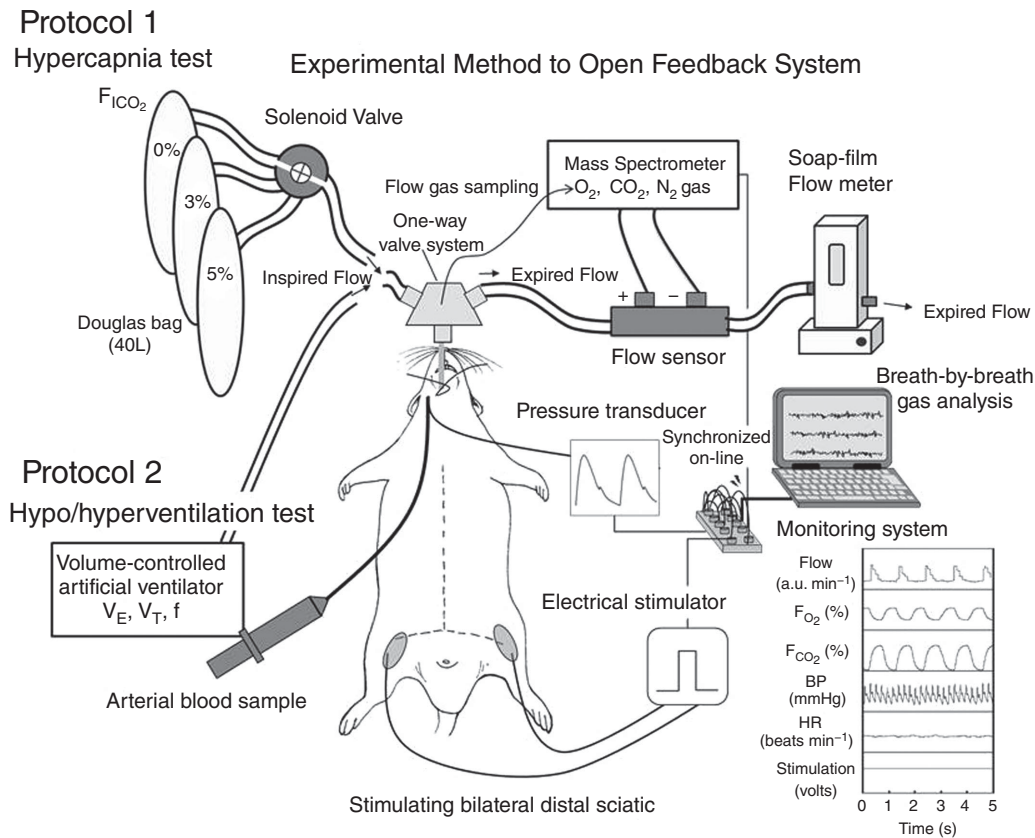
FIGURE 2 Experimental set-up used for characterizing the respiratory chemoreflex feedback system in an anaesthetized rat. We recorded breath-by-breath gas analysis data during electrically induced exercise at low and high voltage, while running two protocols to characterize the controller [protocol 1, hypercapnia test: end-tidal CO_2 tension (P_{ETCO_2}) to $\dot{V}_E$ relationship] and plant (protocol 2, hypo/hyperventilation test: $\dot{V}_E$ to P_{ETCO_2} relationship) of the respiratory system at rest and during electrically induced exercise. f, respiratory rate; F_{ICO_2}, fractional concentration of inspired CO_2; V_T, tidal volume

the controller are equivalent to central chemosensitivity, and those of the plant correspond to pulmonary efficiency. Since both relationships share common variables, $\dot{V}_E$ and P_{aCO_2}, the intersection of the two curves represents the operating point of the ventilatory response under the closed-loop condition (Figure 1b).

2.6 | Experimental procedures

In order to characterize the controller and plant elements at rest and during stimulation of bilateral distal sciatic nerves under anaesthesia in rats, a hypercapnia test (protocol 1) and a hypo/hyperventilation test (protocol 2) were conducted on two different days.

2.6.1 | Protocol 1. Hypercapnia test: controller system characterization

To characterize the controller, we changed P_{ETCO_2} in 12 anaesthetized normal rats with preserved spontaneous breathing (body weight, 429 ± 42 g). The rats inspired a normoxic gas mixture with increasing inspiratory CO_2 fraction through a ventilatory circuit equipped with a one-way valve. By this method, we induced hypercapnia in the rats. A hypercapnia test was performed to characterize the controller elements by measuring steady-state $\dot{V}_E$. This test consisted of three
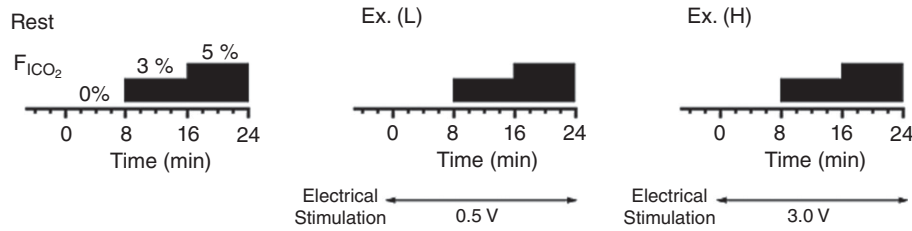
separate trials with different F_{ICO_2} (F_{ICO_2} = 0.00, 0.03 and 0.05; F_{IO_2} = 0.21 with N_2 balance) each under resting and low- and high-intensity mimicked exercise conditions (Figure 3). Baseline data were recorded at F_{ICO_2} = 0.00, before starting the hypercapnia test. Each F_{ICO_2} trial lasted 8 min. The F_{ICO_2} in the inspiration gas was increased stepwise every 8 min, and $\dot{V}_E$ was plotted against P_{ETCO_2}. After completing each hypercapnia test under each condition followed by a 'CO$_2$ washout' period of 20 min, and confirming that values for $\dot{V}_E$ and P_{ETCO_2} had returned to pre-test baseline values, the next hypercapnia test was performed (Figure 4a).

2.6.2 | Protocol 2. Hypo/hyper ventilation test: plant system characterization

To characterize the plant, we altered $\dot{V}_E$ by changing the setting of the artificial ventilator in another 12 normal rats (body weight, 446 ± 32 g). The hypo/hyperventilation test was performed to characterize the plant elements by measuring steady-state P_{ETCO_2} responses to hypo/hyperventilation. Each hypo/hyperventilation test consisted of three trials (1 hypoventilation trial and 2 hyperventilation trials) at resting and exercising conditions (Figures 3 and 4b). For hyperventilation trials, tidal volume and respiratory frequency (respiratory pattern) were predetermined to match those obtained in protocol 1,
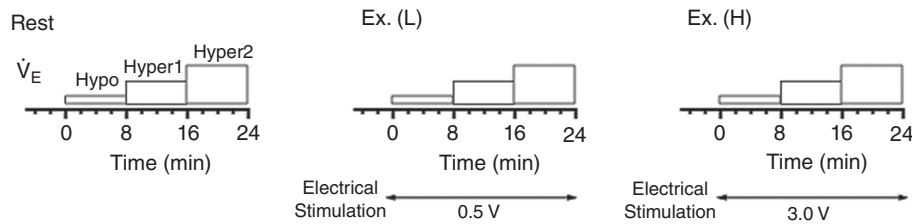
FIGURE 3 Experimental protocols. Protocol 1: the hypercapnia test consisting of 3 separate fractional concentrations of inspired CO_2 (F_{ICO_2}) trials (F_{ICO_2} = 0.00, 0.03 and 0.05, F_{IO_2} = 0.21 with N_2 balance) at rest and during electrically induced exercise. Protocol 2: the hypo/hyperventilation test consisting of 3 trials (1 hypoventilation trial and 2 hyperventilation trials) under resting and exercising conditions. Ex (L), induced low-intensity exercise; Ex (H), induced high-intensity exercise; Rest, resting (no induced exercise)

in order to match the effect of dead volume (Figure 5). For the hypoventilation trial, we altered $\dot{V}_E$ by setting both tidal volume and respiratory frequency 3% lower than the values for the 0.00 F_{ICO_2} condition. After stabilization, we measured the baseline steady-state P_{ETCO_2}. We then altered $\dot{V}_E$ level stepwise and plotted P_{ETCO_2} against $\dot{V}_E$. Each trial lasted 8 min. All trials were performed under normoxic conditions (F_{ICO_2} = 0.00; F_{IO_2} = 0.21 with N_2 balance). A 20 min recovery period of room air breathing was set before each increase in exercise intensity.

2.7 | Assessment of respiratory equilibrium diagram and arterial blood samples

On a separate day, we verified the validity of using steady-state P_{ETCO_2} as a surrogate for P_{aCO_2} throughout the hypercapnic and hypocapnic range under the resting condition in five anaesthetized rats (body weight, 493 ± 38 g). In each rat, we positioned a catheter in the carotid artery to obtain arterial blood samples without stasis. The experiment started 20–30 min after catheter placement. Four hypercapnia tests (F_{ICO_2} = 0.00, 0.03, 0.06 and 0.09; F_{IO_2} = 0.21 with N_2 balance) and five hypo/hyperventilation tests (1 hypoventilation trial, 1 normal ventilation trial, 3 hyperventilation trials) were conducted in all five rats. For the hypercapnia test, the rats inspired gas with increasing F_{ICO_2} through a ventilatory circuit equipped with a one-way valve. The F_{ICO_2} in the inspiration gas was increased stepwise every 8 min. After completing all of the hypercapnia test followed by a 'washout' period of 30 min, and confirming that values for $\dot{V}_E$ and P_{ETCO_2} have returned to pre-test baseline values, hypo/hyperventilation tests were performed in the same rats. For hypo/hyperventilation tests,

we changed the artificial ventilator settings according to ventilation curves at respiratory rates and tidal volumes mimicking those recorded during the hypercapnia trials. Each trial lasted 8 min. All cardiorespiratory parameters were measured using the same methods as in protocols 1 and 2. An arterial blood sample (90 μl) was collected during the last 2 min of each steady-state trial.

Thereafter we characterized the controller and plant elements, and thus ventilatory regulation, by the respiratory chemoreflex system using an equilibrium diagram. The measured values of the operating point in each rat were defined to be the steady-state values for $\dot{V}_E$ and P_{ETCO_2} that were obtained during the 0.00 F_{ICO_2} trial (during spontaneous breathing).

2.8 | Data analysis

In each protocol, steady-state cardiorespiratory data were obtained by averaging the respective data for the last 2 min of each experimental duration. In protocol 1, to characterize the controller system, we performed linear regression of $\dot{V}_E$ against P_{ETCO_2} [$\dot{V}_E = S \times (P_{ETCO_2} - B)$, where S is the slope and B is the P_{ETCO_2} intercept]. In protocol 2, to characterize the plant system, we fitted a metabolic hyperbola ($P_{ETCO_2} = A/\dot{V}_E + C$, where A is the numerator and C is the asymptote of the modified metabolic hyperbola (see Appendix), modified from the original metabolic hyperbola, to the measured data including normal spontaneous breathing data. The operating points obtained at rest and during electrically induced exercise were defined as the steady-state values of $\dot{V}_E$ and P_{ETCO_2} obtained in the trial of F_{ICO_2} = 0.00 (during spontaneous breathing) of the hypercapnia test in protocol 1 (Table 1). The plant gain (G_P) was calculated as the

(a) Protocol 1

Hypercapnia test

(b) Protocol 2
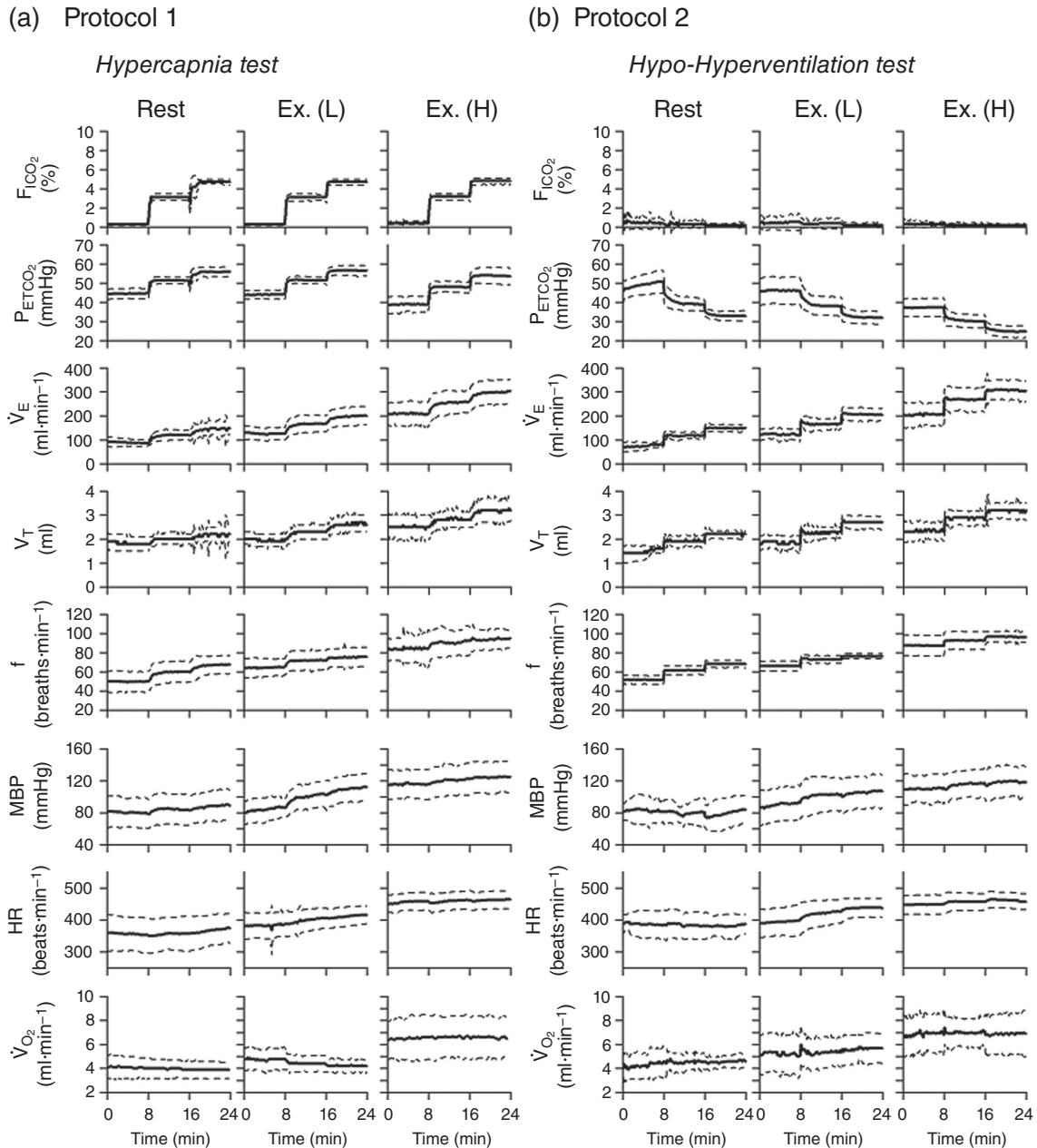
Hypo-Hyperventilation test

FIGURE 4 Time courses of cardiorespiratory responses at rest and during electrically induced exercise at low and high intensities in the hypercapnia test (a; protocol 1) and in the mechanical hypo- and hyper-ventilation test (b; protocol 2). f, respiratory rate; HR, heart rate; MBP, mean blood pressure; P_{ETCO_2}, end-tidal CO_2 partial pressure; $\dot{V}_E$, minute ventilation; $\dot{V}_{O_2}$, oxygen uptake; V_T, tidal volume. Bold continuous lines represent the mean, and dashed lines indicate $\pm$ SD

reciprocal of the slope of the modified metabolic hyperbola at the operating point. The total loop gain at the operating point (G_{Total}) was estimated by the product of the gains of the controller and the plant.

2.9 | Statistical analysis

In each protocol, depending on the purpose of comparison, one-way, factorial and repeated measures ANOVA followed by Tukey's test were conducted on each response variable using mean data of an individual rat. Fitted parameters for the controller and plant elements were obtained by fitting response curves using linear and non-linear

least-squares regression analysis. Pearson's product-moment correlations were calculated between P_{ETCO_2} and P_{aCO_2} values. Comparisons between P_{aCO_2} and P_{ETCO_2} measures were also evaluated using Bland–Altman analysis (Bland & Altman, 1986). The Bland–Altman plot was subsequently analysed by linear regression analysis to determine if the slope of the relationship was greater than zero, which would indicate that a proportional bias was present (i.e. the difference between two methods changes as the average values from the two methods becomes smaller or larger). Furthermore, a fixed bias is present if the 95% confidence limit of the Bland–Altman plot does not include zero. All data are presented as the mean $\pm$ SD and significance for all two-tailed tests was set at $P < 0.05$.

TABLE 1 Cardiorespiratory parameters (data averaged over the last 2 min of each trial) at the operating points during the pre-experimental baseline period in each protocol, and during experimental periods at rest and during mimicked exercise in protocol 1

Parameter	Pre-experimental baseline (F_{ICO_2} = 0.0%)		Experimental trial periods in protocol 1 (F_{ICO_2} = 0.0%); data at operating points		
	Protocol 1 (n = 12)	Protocol 2 (n = 12)	Rest (n = 12)	Ex (L) (n = 12)	Ex (H) (n = 12)
P_{ETCO_2} (mmHg)	44.2 ± 2.8	43.9 ± 4.1	44.6 ± 2.7	44.1 ± 2.4	38.9 ± 4.0**,††
$\dot{V}_E$ (ml min^{-1})	77.0 ± 26.4	79.5 ± 25.1	83.0 ± 13.3	124 ± 19**	204 ± 45**,††
V_T (ml)	1.6 ± 0.9	1.6 ± 0.5	1.7 ± 0.2	1.9 ± 0.2*	2.4 ± 0.3**,††
f (breaths min^{-1})	50.1 ± 11.3	51.5 ± 8.3	49.8 ± 10.8	65.0 ± 8.8**	84.4 ± 16.5**,††
$\dot{V}_{O_2}$ (ml min^{-1})	3.4 ± 1.2	3.3 ± 1.0	3.7 ± 0.7	4.7 ± 0.7**	6.4 ± 1.2**,††
$\dot{V}_{CO_2}$ (ml min^{-1})	2.8 ± 1.0	2.7 ± 0.8	3.0 ± 0.5	4.2 ± 0.5**	5.7 ± 1.0**,††
MBP (mmHg)	81.8 ± 21.4	79.7 ± 19.8	79.7 ± 19.7	86.9 ± 13.6	116 ± 19**,††
HR (beats min^{-1})	363 ± 58.1	383 ± 38.5	353 ± 56	386 ± 40	460 ± 30**,††

Values are presented as means ± SD. Ex (H), induced high-intensity exercise; Ex (L), induced low-intensity exercise; f, respiratory rate; HR, heart rate; MBP, mean blood pressure; P_{ETCO_2}, end-tidal pressure for CO_2; Rest, resting (no induced exercise); $\dot{V}_{CO_2}$, carbon dioxide output; $\dot{V}_E$, minute ventilation; $\dot{V}_{O_2}$, oxygen uptake; V_T, tidal volume. * $P < 0.05$; ** $P < 0.01$ vs. Rest; †† $P < 0.01$ vs. Ex (L).
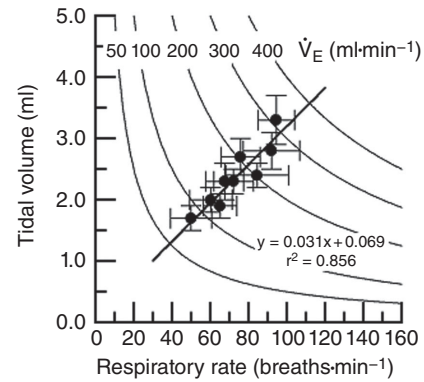

FIGURE 5 The relationship between respiratory rate and tidal volume under spontaneous breathing at rest and during electrically induced exercise at low and high intensities in the hypercapnia test (protocol 1)

3 | RESULTS

Hereinafter, electrically induced muscle contraction mimicking exercise is referred to as exercise. Table 1 shows cardiorespiratory parameters at the operating points during the pre-experimental baseline periods in protocols 1 and 2, and during experimental periods at rest and during muscle contraction induced by electrical stimulation of bilateral distal sciatic nerves at low (0.1–0.5 V) and high voltage (3.0 V) under spontaneous breathing in protocol 1 (F_{ICO_2}; 0.0%). During the baseline period in protocols 1 and 2, there were no significant differences in all cardiorespiratory parameters between protocols 1 and 2. During the experimental period in protocol 1, although P_{ETCO_2} was regulated at constant level causing exercise hyperpnoea, the exercise stimulus induced voltage-dependent increases in all cardiorespiratory and metabolic parameters. ANOVA revealed a significant main effect of exercise intensity for $\dot{V}_E$, tidal volume (V_T), respiratory rate (f), $\dot{V}_{O_2}$, $\dot{V}_{CO_2}$, mean blood pressure (MBP) and heart rate (HR), indicating that electrically induced exercise at higher intensity significantly increased the above parameters compared to the resting state ($P < 0.01$). A *post hoc* analysis revealed that higher exercise intensity increased $\dot{V}_E$, V_T, f, $\dot{V}_{O_2}$, $\dot{V}_{CO_2}$, MBP and HR, and decreased P_{ETCO_2} ($P < 0.01$) (Table 1).

Figure 4 shows the averaged data of the time courses of cardiorespiratory responses at rest and during electrically induced exercise in the hypercapnia test (protocol 1) and the mechanical hypo- and hyperventilation test (protocol 2). In the hypercapnia test both at rest and during exercise at low and high intensities, stepwise increase of F_{ICO_2} from 0 to 0.05 was accompanied by increases of P_{ETCO_2}, $\dot{V}_E$, V_T and f at each F_{ICO_2} increase, reaching steady states in 3–6 min (Figure 4a). Figure 4b illustrates the effects of changes in $\dot{V}_E$ on cardiorespiratory parameters at rest and during electrically induced exercise at low and high intensities. Hypoventilation increased P_{ETCO_2} while hyperventilation decreased P_{ETCO_2}, and the changes reached steady states in 6–8 min in each trial both at rest and during exercise (Figure 4b).

Figure 5 shows the relationships between respiratory rate and tidal volume during spontaneous breathing in the hypercapnia test both
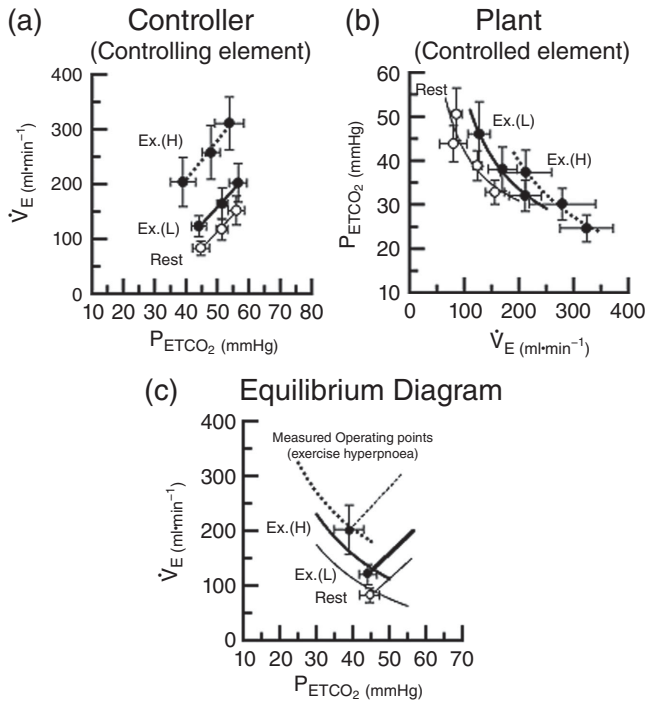
FIGURE 6 Characteristics of the controller (a) and the plant (b) systems at rest and during electrically induced exercise at low and high intensity. Exercise intensity-dependent changes in operating points ($\dot{V}_E$ and P_{ETCO_2}) were estimated by integrating the controller and plant curves in a respiratory equilibrium diagram (c)

TABLE 2 Parameters of controller and plant properties, and respiratory total loop gain at rest and during electrically induced exercise at low and high intensities

Parameter	Rest	Ex (L)	Ex (H)
Controller ($n = 12$)			
S (ml min^{-1} mmHg^{-1})	6.2 ± 2.0	6.4 ± 2.1	7.2 ± 2.7
B (mmHg)	30.7 ± 5.6	$23.4 \pm 6.6^*$	$-2.5 \pm 52.1^{**}$
Plant ($n = 12$)			
A (ml min^{-1} mmHg^{-1})	2440 ± 627	$4252 \pm 1306^{**}$	$7389 \pm 2044^{**,\dagger\dagger}$
C (mmHg)	18.0 ± 6.1	$12.1 \pm 4.7^*$	$2.8 \pm 4.7^{**,\dagger\dagger}$
G_P (mmHg ml^{-1} min^{-1})	0.36	0.26	0.18
G_{Total}	2.0	1.6	1.3

Values are expressed as means $\pm$ SD. Controller: $\dot{V}_E = S \times (P_{ETCO_2} - B)$; S, controller gain; B, P_{ETCO_2} intercept. Plant: $P_{ETCO_2} = A/\dot{V}_E + C$. A is the numerator and C is the asymptote of the modified metabolic hyperbola. Ex (H), induced high-intensity exercise; Ex (L), induced low-intensity exercise; G_P, plant gain at operating point; G_{Total}, total loop gain at operating point; Rest, resting (no induced exercise). $^*P < 0.05$; $^{**}P < 0.01$ vs. Rest; $^{\dagger\dagger}P < 0.01$ vs. Ex (L).

at rest and during exercise in protocol 1. There were no significant differences in the breathing pattern (V_T vs. f relationship) during all trials for both resting and exercise conditions.

Figure 6 shows the characteristics of the controller and the plant at rest and during electrically induced exercise obtained from the averaged steady-state data shown in Figure 4a and b. For the controller curve, $\dot{V}_E$ increased linearly with increase in P_{ETCO_2} at rest and during exercise ($r^2 = 0.808$–0.995; pooled data of all rats) (Figure 6a). The plant curve approximated the modified metabolic hyperbola reasonably well ($r^2 = 0.962$–0.996; all rats) (Figure 6b). Table 2 shows the estimated parameters of the controller and plant properties, and respiratory total loop gain at rest and during electrically induced exercise at low and high intensities. For the controller, the regression line of the $\dot{V}_E$–P_{aCO_2} relationship shifted upward depending on exercise intensity without significant change in controller gain (S). ANOVA revealed that a significant main effect was observed for the P_{ETCO_2} intercept (B) ($F_{[2,22]} = 3.94$, $P = 0.035$). A post hoc analysis revealed that the P_{ETCO_2} intercept (B) during electrically induced high- and low-intensity exercise was markedly reduced compared to the resting condition, but there was no difference between both intensities (Table 2). The fitted plant curve shifted rightward and downward depending on exercise intensity as predicted by increase in metabolic rate (Figure 6b). ANOVA revealed that a significant main effect was observed for the numerator A of the modified metabolic hyperbola ($F_{[2,22]} = 35.80$, $P < 0.001$) and also for the asymptote parameter C ($F_{[2,22]} = 20.02$, $P < 0.001$). A post hoc analysis revealed that electrically induced high- and low-intensity exercise significantly increased A and

decreased C compared to resting condition. Furthermore, both A and C values showed a significant difference between both intensities (Table 2).

The respiratory equilibrium diagram was constructed by plotting the controller and plant curves together on the same graph, at rest and during electrically induced exercise at low and high intensities (Figure 6c). The intersecting point between the controller and plant curves predicts the closed-loop respiration operating point. Induced exercise shifted the operating point upward, which effectively stabilized P_{ETCO_2} within the normal range, and decreased the plant gain (G_P) calculated by the reciprocal of the slope of the modified metabolic hyperbola at the operating point, while the controller gain remained unchanged (S) (Table 2). The significant main effect indicated that the absolute value of G_P at low-intensity exercise was smaller than at high-intensity exercise. The estimated total loop gain at the operating point (product of the controller and plant gain) was lower at high-intensity exercise.

In five rats, the relationships between steady-state P_{ETCO_2} and P_{aCO_2} for four F_{ICO_2} trials as well as one hypoventilation, one normal ventilation and three hyperventilation trials are illustrated in Figure 7. P_{ETCO_2} correlates tightly with P_{aCO_2} ($n = 45$, $P_{aCO_2} = 0.928 \times P_{ETCO_2} + 4.8$, $r^2 = 0.910$, $P < 0.001$) throughout the hypercapnic and hypocapnic range under the resting condition, but P_{ETCO_2} consistently under-estimates P_{aCO_2} (Figure 7a). In addition, a one-way repeated-measures ANOVA revealed no difference between measured values of P_{ETCO_2} (48.5 ± 16.7 mmHg) and P_{aCO_2} (49.8 ± 16.2 mmHg). For the Bland–Altman plot, there was a small bias between measurement devices (bias, -1.3 mmHg) and 95% confidence limits of -11.1 and 8.5 mmHg (Figure 7b).

Furthermore, we characterized the controller ($S = 8.9 \pm 2.5$ ml min^{-1} mmHg^{-1}, $B = 29.4 \pm 2.7$ mmHg) and plant elements ($A = 3398 \pm 851$ ml min^{-1} mmHg^{-1}, $C = 13.6 \pm 1.7$ mmHg) in each
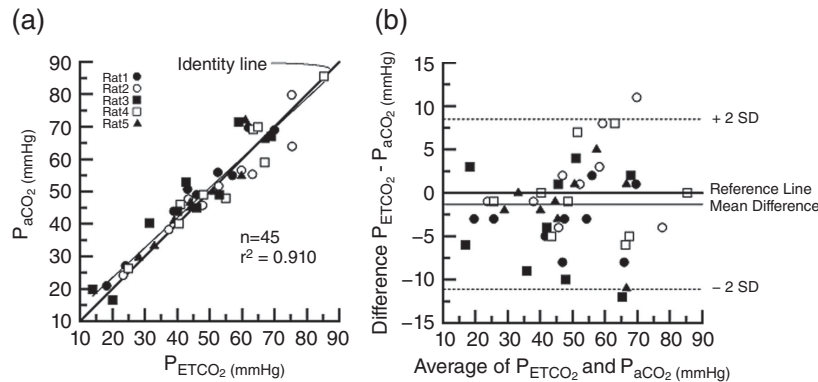
FIGURE 7 The relationships between steady-state P_{ETCO_2} and P_{aCO_2} for 4 F_{ICO_2} trials as well as 1 hypoventilation, 1 normal ventilation and 3 hyperventilation trials in five rats. P_{ETCO_2} correlates tightly with P_{aCO_2} ($n = 45$, $P_{aCO_2} = 0.928 \times P_{ETCO_2} + 4.8$, $r^2 = 0.910$, $P < 0.001$) throughout the hypercapnic and hypocapnic range under resting condition. Measures of P_{ETCO_2} (48.5 ± 16.7 mmHg) and P_{aCO_2} (49.8 ± 16.2 mmHg) were similar, but P_{ETCO_2} consistently underestimates P_{aCO_2}. The linear regression analysis (a) and the Bland–Altman plot (b) also revealed a close relationship between P_{aCO_2} and P_{ETCO_2}. For the Bland–Altman plot, there was a small bias between measurement devices (bias, -1.3 mmHg) and 95% confidence limits of -11.1 and 8.5 mmHg. Different symbols represent results from individual rats ($n = 5$). A regression analysis was performed on pooled data. Bold line, identity line; fine line, linear regression

rat. Their operating points estimated by the equilibrium diagram (the intersection between the two relationship lines) were very close to those during closed-loop spontaneous breathing. Consequently, mean estimated P_{ETCO_2} and $\dot{V}_E$ values at the operating point were statistically indistinguishable from the measured values (42.9 ± 3.0 *vs.* 42.8 ± 2.8 mmHg, and 112.7 ± 11.5 *vs* 110.4 ± 9.8 ml•min^{-1}, respectively). The gain of the plant estimated by the reciprocal of the slope of the hyperbola curve at the operating point was 0.30 ± 0.07 mmHg ml^{-1} min^{-1}. The estimated total loop gain at the operating point, i.e. the product of the gains of the controller and the plant, was 2.6 ± 0.3.

4 | DISCUSSION

The present study clearly showed that exercise intensity-dependent increases in cardiorespiratory responses are adjusted to $\dot{V}_{O_2}$ increase by evoking muscular activity through electrical stimulation of the peripheral ends of severed bilateral sciatic nerves. Furthermore, under each experimental condition in spontaneously breathing anaesthetized rats (Table 1), the absolute values of $\dot{V}_E$ and averaged breathing pattern (V_T–RR relationship in Figure 5) were well within the range reported by Crosfill & Widdicombe (1961) and Palecek et al. (1969). In addition, we experimentally demonstrated that exercise hyperpnoea, i.e. normal isocapnic ventilatory response to electrically induced exercise, can be determined by integrating the controller and plant properties in the respiratory equilibrium diagram.

4.1 | Interpretation of the operating point of respiration using the respiratory equilibrium diagram

In this study, electrically stimulated exercise shifted the plant curve rightward and upward, reflecting increased metabolism ($\dot{V}_{CO_2}$ increase). If the exercise stimulus had not affected the controller

element, the operating point during exercise would have been the intersecting point between the fine straight line and the bold hyperbola in Figure 6c. In that case, P_{ETCO_2} would have increased to above 50 mmHg. However, the electrically induced exercise can produce an isocapnic ventilatory response. These results show that the exercise stimulus shifts the controller element toward higher $\dot{V}_E$, which effectively stabilizes P_{ETCO_2} within the normal range, at the expense of exercise hyperpnoea (Figure 6c).

Several decades ago, Cunningham et al. (1986) proposed a model of chemoreflex control of respiration at rest and during exercise. The concept of using the respiratory equilibrium diagram has also been proposed by Berger et al. (1977), Folgering (1988) and Mahamed, Ali, Ho, Wang, & Duffin (2001), Milhorn (1966). Previously, we have demonstrated that the operating point of respiration at rest and during exercise can be described by the point of intersection of the controller and plant curves in the respiratory equilibrium diagram in humans (Miyamoto et al., 2004, 2012, 2014, 2015, Ogoh et al., 2008). In the present investigation using anaesthetized small animals, we succeeded in characterizing these subsystem under an open-loop condition and constructed a respiratory equilibrium diagram to illustrate the mechanisms of respiratory regulation at rest and during electrically induced exercise. Therefore, the present investigation extends previous animal studies of respiratory control by demonstrating the exercise intensity-dependent shift of the operating points in the respiratory equilibrium diagram. Indeed, the operating P_{ETCO_2} and $\dot{V}_E$ estimated from the intersection point on the respiratory equilibrium diagram conformed reasonably well to the values actually measured regardless of rest and exercise conditions (Figure 6c).

4.2 | Exercise-induced shift in the controller element

In the present study, we found that the controller curve shifts upward to compensate for the plant curve shift accompanying increased metabolism. Furthermore, the exercise stimulus did not change the controller gain (S) despite an increase in metabolic demand. However,

the P_{ETCO_2} intercept (B) during electrically induced high-intensity exercise was smaller compared to resting and low-intensity exercise conditions, indicating that the exercise-induced upward shift of the controller curve was exercise intensity-dependent (Table 2; Figure 5).

As verified in the present study, many physiologists concur on the exercise-induced upward shift of the controller curve in both humans (Clark, Sinclair, & Lenox, 1980; Duffin et al., 1980; Miyamoto et al., 2012; Ogoh et al., 2008; Weil et al., 1972) and anaesthetized mammals (Asmussen, 1957, 1965; Kao, 1963), although the effect of exercise stimulus on the controller gain (CO_2 sensitivity) varies among studies.

In a human study, Casey, Duffin, and McAvoy (1987) demonstrated that exercise did not change the central chemoreceptor threshold, supporting the neuro-humoral theory of exercise ventilation. The concept of an additional drive to breathe during exercise apart from the chemoreflex is now considered common knowledge. These findings thus suggest that the additional drive to breathe during exercise is greater at high-intensity exercise, which is not necessarily due to a change in central chemoreflex threshold.

Despite almost 100 years of intensive study, the pathways that mediate exercise hyperpnoea have not been clearly defined (Eldridge, 1994; Eldridge & Waldrop, 1991; Kao, 1963; Krogh & Lindhard, 1913; Mateika & Duffin, 1995; Strange et al., 1993; Wasserman et al., 1986; Forster et al., 2012). As a result, a fundamental conflict seems to exist in the literature on exercise hyperpnoea, and a variety of mechanisms have been postulated to explain the exercise-induced upward shift of the controller curve during exercise, which leads to exercise hyperpnoea.

In this experimental study, although the drives to breathe in addition to the chemoreflex drive have not been defined, the neural drives originating from the central and peripheral nervous system (Forster et al., 2012); afferents from the working limbs (Comroe & Schmidt, 1943; Kao, 1963; McCloskey & Mitchell, 1972; Smith, Mitchell, & Garry, 2006) and afferents from the heart (Wasserman, Whipp, & Castagna, 1974, Wasserman, Whipp, & Casaburi, 1986) may be involved in the exercise-induced upward shift of the controller curve, leading to exercise hyperpnoea. Recent findings that support critical contributions from cortical central command and muscle afferent feedback to exercise hyperpnoea are reviewed (Forster et al., 2012). On the other hand, in our current model, despite the absence of the central command, the fact that involuntary muscle activation was sufficient to elicit isocapnic exercise hyperpnoea indicated that central motor activity/central command does not contribute to the hyperpnoea under this experimental condition. Brice et al. (1988) also indicated that central command is not requisite for the precise matching of alveolar ventilation to increases in $\dot{V}_{CO_2}$ during low-intensity muscle contractions in humans. Although their study limitation is that 50–100% increase in metabolic rate is within the physiological variation that occurs at rest, their results were consistent with our findings.

4.3 | Exercise-induced shift in the plant element

In the present study, exercise induced by electrical stimulation shifted the plant curve rightward and downward reflecting increased metabolism, and the exercise intensity-dependent changes in the plant element is characterized by an increase in A and a decrease in C (Appendix, Equation (2)).

In the past, some researchers have explained the exercise-induced changes in the plant element using the conventional metabolic hyperbola (Wasserman et al., 1986; Whipp & Pardy, 1986). In the conventional method, the equation that expresses the relation between $\dot{V}_E$ and P_{aCO_2} during exercise ignores the scaling factors representing ventilatory work-related CO_2 production. However, because ventilatory work-related CO_2 production occurs and V_D/V_T changes with variation in $\dot{V}_E$ in 'real-life' physiological systems (Aaron, Seow, Johnson, & Dempsey, 1992; Crosfill & Widdicombe, 1961; Harms, Wetter, St Croix, Pegelow, & Dempsey, 2000), we modified the conventional metabolic hyperbola to explain the exercise-induced changes in plant element (see Appendix). In the modified metabolic hyperbola ($P_{ETCO_2} = A/\dot{V}_E + C$), the increase in A may result from increases in basal metabolic demand (α) and/or V_D/V_T (Appendix, Equation (3)). The decrease in C may result from decreases in V_D/V_T and/or metabolic cost of breathing (β) (Appendix Equation (3); Miyamoto et al., 2004). V_D/V_T is unlikely to increase during exercise, because the exercise stimulus increases V_T but decreases V_D due to improved $\dot{V}_A/\dot{Q}$ mismatch. Therefore, β probably decreases accompanying reduced airway resistance, consequently reducing the oxygen cost of breathing. On the other hand, exercise intensity-dependent increase in A may be mainly due to increase in basal metabolic demand and decrease in C, which decrease both V_D/V_T and β. Therefore, plant system characteristics curves obtained show unique changes according to given conditions. Although we did not evaluate such physiological measurement in this experiment, these 'metabolic factors' (A and C) may explain the leftward shift of the operating point during electrically induced exercise at high intensity (Figure 6c).

In the living body, since the input–output relationship is finally determined according to many elements including the anatomical and physiological dead space [respiratory pattern, ventilation to perfusion ratio ($\dot{V}_A/\dot{Q}$) mismatch], airway resistance and CO_2 output (metabolic level), an accurate description of the functional characteristics of the plant system can be important, especially in patients with cardio-pulmonary lesions. Therefore, this diagram can be useful in understanding not only the mechanism of respiratory control at rest and during exercise, but also the pathophysiological mechanism of diseases manifesting breathing disorders.

4.4 | Clinical perspectives

We demonstrated that respiration is determined from the inter-secting point of the controller and the plant curves on the respiratory equilibrium diagram. Consequently, the quantitative analysis of the two subsystems of respiratory chemoreflex provides a framework by which we can analytically evaluate how the unique value of $\dot{V}_E$ during exercise is determined by the respiratory chemoreflex system, how changes in model parameters of controller (S and B) and plant (α, β, A, and C) elements affect exercise hyperpnoea. Using this conceptual diagram, it is possible to analytically estimate

with high precision whether (abnormal) changes of the controlling element and the controlled element cause (abnormal) changes in $\dot{V}_E$ and P_{aCO_2}, or conversely, how (abnormal) changes in $\dot{V}_E$ and P_{aCO_2} alter the characteristics of the system. Indeed, we have already constructed a respiratory equilibrium diagram to illustrate the respiratory abnormalities in CHF rats under anaesthesia, and suggested the potential difference between normal and CHF rats in exercise-induced changes in controller and plant (Miyamoto et al., 2006). Therefore, using this experimental model, systematic evaluation of their integrated function would also help elucidate the pathophysiological key mechanisms responsible for controlling ventilation.

In the future, quantitative analysis of the dynamic properties of the respiratory chemoreflex system may play a role in elucidating the adaptive mechanism of the exercise ventilatory response during training and the mechanism of respiratory abnormality in CHF. The mechanisms of their occurrence have been attributed to a change in sensitivity to carbon dioxide (gain) or an increase in lung-chemoreceptor circulation time associated with central respiratory disorder. Especially, in CHF patients, the increase in central and peripheral chemoreflex sensitivity (controller gain) and the increase in peripheral plant gain because of an increase in dead space/tidal volume ratio are speculated to cause a total loop gain increase in the system.

4.5 | Experimental limitations

There are several limitations to the present study. First, we obtained data from anaesthetized animals. If data had been obtained from conscious animals, the results might have been different. However, because human studies have observed the same exercise-induced upward shift of the controller curve during exercise, which leads to exercise hyperpnoea (Miyamoto et al., 2012; Ogoh et al., 2008), the interpretation of the observed changes in the operating points may be reasonable. Second, the present study consistently showed that electrical stimulation to involuntarily contract skeletal muscles in rats increases mean arterial pressure, heart rate and ventilation. Some components of this constellation of responses to involuntary contraction may be the result of the reflex arising either from the working muscles or from direct activation of afferent fibres. Alternatively, a metabolic byproduct of involuntary muscular contraction may have circulated to other regions such as the lung and carotid bodies to evoke these responses. Although there is a paucity of data concerning the effects of possible abnormal sensory stimulation resulting from electrically induced exercise, our result in general agrees with other physiological studies using direct electrical stimulation to evoke muscular activity, which has been widely used in anaesthetized mammals (Kao, 1963; Lamb, 1966; Linton, Miller, & Cameron, 1976; Waldrop, Mullins, & Millhorn, 1986). In addition, our quantitative observation of isocapnic ventilatory response and intensity-dependent change in the controller and plant elements during exercise may be evidence that neural and/or metabolic factors account for the isocapnic exercise hyperpnoea. Third, in the present study, the estimation of P_{aCO_2} using P_{ETCO_2} may have limitations. However, our validation experiment revealed that P_{ETCO_2} correlated closely with P_{aCO_2} ($n = 45$, $P_{aCO_2} = 0.93 \times P_{ETCO_2} + 4.8$, $R^2 = 0.910$, $P < 0.001$) (Figure 5a). Therefore, the change in P_{ETCO_2} observed during experimental conditions likely reflects P_{aCO_2}. However, P_{ETCO_2} was shown to slightly underestimate P_{aCO_2} across all experimental conditions, a finding that is consistent with a previous report (Jones, Robertson, & Kane, 1979). Furthermore, Jones and Campbell (1982) reported that P_{ETCO_2} is higher than P_{aCO_2} when F_{ICO_2} and $\dot{V}_E$ increase, but is lower under normal conditions. Therefore, the values of controller gain, plant gain and total loop gain may be underestimated using P_{ETCO_2} as a surrogate for P_{aCO_2}. Finally, another limitation is that to characterize the plant element, the rats were subject to non-physiological respiration using a mechanical ventilator, which might have affected the P_{ETCO_2} response to $\dot{V}_E$. However, the combinations of tidal volume and respiratory frequency were predetermined in order to match the spontaneous breathing pattern, because we tried to match the effect of dead volume as well. Thus, our conceptual interpretation of the observed changes in plant system properties, and assessment of the respiratory equilibrium diagram are likely to be valid.

5 | CONCLUSIONS

We developed an anaesthetized-rat model for studying exercise hyperpnoea during electrically induced muscular contraction, using systems analysis for quantitative characterization of the respiratory chemoreflex feedback system. This small-animal experimental model will provide an opportunity to clarify the major determinant mechanisms of exercise hyperpnoea, and will be useful for understanding the mechanisms responsible for abnormal ventilation under various pathophysiological conditions.

COMPETING INTERESTS

None declared.

AUTHOR CONTRIBUTIONS

Conception or design of the work: T.M. Acquisition, analysis, or interpretation of data for the work: T.M., K.M., S.U., H.N. Drafting the work or revising it critically for important intellectual content: T.M. All authors approved the final version of the manuscript and agree to be accountable for all aspects of the work in ensuring that questions related to the accuracy or integrity of any part of the work are appropriately investigated. All persons designated as authors qualify for authorship, and all those who qualify for authorship are listed.

ORCID

Tadayoshi Miyamoto http://orcid.org/0000-0001-5504-6119

REFERENCES

Aaron, E. A., Seow, K. C., Johnson, B. D., & Dempsey, J. A. (1992). Oxygen cost of exercise hyperpnea: Implications for performance. *Journal of Applied Physiology*, *72*, 1818–1825.

Ainslie, P. N., & Duffin, J. (2009). Integration of cerebrovascular CO_2 reactivity and chemoreflex control of breathing: Mechanisms of regulation, measurement, and interpretation. *American Journal of Physiology. Regulatory, Integrative and Comparative Physiology*, *296*, R1473–R1495.

Arzt, M., Harth, M., Luchner, A., Muders, F., Holmer, S. R., Blumberg, F. C., … Pfeifer, M. (2003). Enhanced ventilatory response to exercise in patients with chronic heart failure and central sleep apnea. *Circulation*, *107*, 1998–2003.

Asmussen, E., & Nielsen, M. (1957). Ventilatory response to CO_2 during work at normal and at low oxygen tensions. *Acta Physiologica Scandinavica*, *39*, 27–35.

Asmussen, E. (1965). Muscular exercise. In Fenn, W. O. & Rahn, H. (Eds.), *Handbook of physiology*, section 3, *Respiration*, vol. II (pp. 631–648). Washington, DC: American Physiological Society.

Bassols, A. M., Carreras, J., & Cussó, R. (1986). Changes in glucose 1,6-bisphosphate content in rat skeletal muscle during contraction. *Biochemical Journal*, *240*, 747–751.

Berger, A. J., Mitchell, R. A., & Severinghaus, J. W. (1977). Regulation of respiration (third of three parts). *The New England Journal of Medicine*, *297*, 194–201.

Bin-Jaliah, I., Maskell, P. D., & Kumar, P. (2005). Carbon dioxide sensitivity during hypoglycaemia-induced, elevated metabolism in the anaesthetized rat. *The Journal of Physiology*, *563*, 883–893.

Bland, J. M., & Altman, D. G. (1986). Statistical methods for assessing agreement between two methods of clinical measurement. *Lancet*, *1*, 307–310.

Brice, A. G., Forster, H. V., Pan, L. G., Funahashi, A., Lowry, T. F., Murphy, C. L., & Hoffman, M. D. (1988). Ventilatory and P_{aCO2} responses to voluntary and electrically induced leg exercise. *Journal of Applied Physiology*, *64*, 218–225.

Casey, K., Duffin, J., & McAvoy, G. V. (1987). The effect of exercise on the central-chemoreceptor threshold in man. *The Journal of Physiology*, *383*, 9–18.

Clark, J. M., Sinclair, R. D., & Lenox, J. B. (1980). Chemical and nonchemical components of ventilation during hypercapnic exercise in man. *Journal of Applied Physiology*, *48*, 1065–1076.

Comroe, J. H., & Schmidt, C. F. (1943). Reflexes from the limbs as a factor in the hyperpnea of muscular exercise. *American Journal of Physiology*, *138*, 536–547.

Crosfill, M. L., & Widdicombe, J. G. (1961). Physical characteristics of the chest and lungs and the work of breathing in different mammalian species. *The Journal of Physiology*, *158*, 1–14.

Cummin, R. C., & Saunders, K. B. (1987). The ventilatory response to inhaled CO_2. In Whipp, B. J. (Ed.), *The control of breathing in man* (pp. 45–67). Manchester: Manchester University Press.

Cunningham, D. J. C., Robbins, P. A., & Wolff, C. B. (1986). Integration of respiratory responses to changes in alveolar partial pressures of CO_2 and O_2 and in arterial pH. In Cherniack, N. S. & Widdicombe, J. (Eds.), *Handbook of physiology*, section 3, *The respiratory system*, vol. II, *Control of breathing* (pp. 475–528). Bethesda, MD: American Physiological Society.

Defares, J. G. (1964). Principles of feedback control and their application to the respiratory control system. In Fenn, W. O. & Rahn, H. (Eds.), *Handbook of physiology*, section 3, *Respiration*, vol. I (pp. 649–680). Bethesda, MD: American Physiological Society.

Dempsey, J. A., Miller, J. S., & Roman, L. M. (2006). The respiratory system. In Tipton, C. M., Sawka, C.N., Tate, C.A., & Terjing, R.J. (Eds.), *ACSM's Advanced exercise physiology* (pp. 246–299). Philadelphia: Lippincott, Williams, and Wilkins.

Dempsey, J. A., & Smith, C. A. (2014). Pathophysiology of human ventilatory control. *The European Respiratory Journal*, *44*, 495–512.

Duffin, J., Bechbache, R. R., Goode, R. C., & Chung, S. A. (1980). The ventilatory response to carbon dioxide in hyperoxic exercise. *Respiration Physiology*, *40*, 93–105.

Eldridge, F. L., & Waldrop, T. G. (1991). Neural control of breathing during exercise. In Whipp, B. & Wasserman, K. (Eds.), *Exercise, pulmonary physiology and pathophysiology* (pp. 309–370), New York: Dekker.

Eldridge, F. L. (1994). Central integration of mechanisms in exercise hyperpnea. *Medicine and Science in Sports and Exercise*, *26*, 319–327.

Folgering, H. (1988). Studying the control of breathing in man. *The European Respiratory Journal*, *1*, 651–660.

Forster, H. V., Haouzi, P., & Dempsey, J. A. (2012). Control of breathing during exercise. *Comprehensive Physiology*, *2*, 743–777.

Guazzi, M., Raimondo, R., Vicenzi, M., Arena, R., Proserpio, C., Sarzi Braga, S., & Pedretti, R. (2007). Exercise oscillatory ventilation may predict sudden cardiac death in heart failure patients. *Journal of the American College of Cardiology*, *50*, 299–308.

Hayashi, F., Yoshida, A., Fukuda, Y., & Honda, Y. (1982). CO_2-ventilatory response of the anesthetized rat by rebreathing technique. *Pflügers Archiv*, *393*, 77–82.

Harms, C. A., Wetter, T. J., St Croix, C. M., Pegelow, D. F., & Dempsey, J. A. (2000). Effects of respiratory muscle work on exercise performance. *Journal of Applied Physiology*, *89*, 131–138.

Jones, N. L., Robertson, D. G., & Kane, J. W. (1979). Difference between end-tidal and arterial P_{CO2} in exercise. *Journal of Applied Physiology*, *47*, 954–960.

Jones, N., & Campbell, E. J. M. (Eds.) (1982). *Clinical exercise testing* (pp. 130–151), Philadelphia: WB Saunders Co.

Krogh, A., & Lindhard, J. (1913). The regulation of respiration and circulation during the initial stages of muscular work. *The Journal of Physiology*, *47*, 112–136.

Kao, F. F. (1963). An experimental study of the pathways involved in exercise hyperpnea employing cross-circulation techniques. In Cunningham, D. J. C. & Lloyd, B. B. (Eds.), *Regulation of human respiration* (pp. 461–502). Philadelphia: Davis Company.

Lamb, T. W. (1966). Ventilatory responses to intravenous and inspired carbon dioxide in anesthetized cats. *Respiration Physiology*, *2*, 99–104.

Linton, R., Miller, R., & Cameron, R. (1976). Ventilatory response to CO_2 inhalation and intravenous infusion of hypercapnic blood. *Respiration Physiology*, *26*, 383–394.

Lloyd, B. B., & Cunningham, D. J. C. (Eds.) (1963). Quantitative approach to the regulation of human respiration. *The regulation of human respiration* (pp. 331–349). Oxford, UK: Blackwell Scientific Publications.

Mateika, J. H., & Duffin, J. (1995). A review of the control of breathing during exercise. *European Journal of Applied Physiology*, *71*, 1–27.

Milhorn, H. T. Jr. (1966). *The applications of control theory to physiological systems* (pp. 113–137). Philadelphia: Saunders.

Miyamoto, T., Inagaki, M., Takaki, H., Kawada, T., Yanagiya, Y., Sugimachi, M., & Sunagawa, K. (2004). Integrated characterization of the human chemoreflex system controlling ventilation, using an equilibrium diagram. *European Journal of Applied Physiology*, *93*, 340–346.

Miyamoto, T., Bailey, D. M., Nakahara, H., Ueda, S., Inagaki, M., & Ogoh, S. (2014). Manipulation of central blood volume and implications for

respiratory control function. *American Journal of Physiology. Heart and Circulatory Physiology*, *306*, H1669–H1678.

Miyamoto, T., Inagaki, M., Takaki, H., Kawada, T., Shishido, T., Kamiya, A., & Sugimachi, M. (2012). Adaptation of the respiratory controller contributes to the attenuation of exercise hyperpnea in endurance-trained athletes. *European Journal of Applied Physiology*, *112*, 237–251.

Miyamoto, T., Nakahara, H., Ueda, S., Manabe, K., Kawai, E., Inagaki, M., … Sugimachi, M. (2015). Periodic breathing in heart failure explained by dynamic and static properties of respiratory control. *Clinical Medicine Insights: Cardiology*, *9*, 133–142.

Miyamoto, T., Inagaki, M., Takaki, H., Kamiya, A., Kawada, T., Shishido, T., … Sunagawa, K. (2006). Sensitized central controller of ventilation in rats with chronic heart failure contributes to hyperpnea little at rest but more during exercise. *Conference Proceedings of the IEEE Engineering in Medicine and Biology Society*, *1*, 4627–4630.

Mahamed, S., Ali, A. F., Ho, D., Wang, B., & Duffin, J. (2001). The contribution of chemoreflex drives to resting breathing in man. *Experimental Physiology*, *86*, 109–116.

McCloskey, D. I., & Mitchell, J. H. (1972). Reflex cardiovascular and respiratory responses originating in exercising muscle. *The Journal of Physiology*, *224*, 173–186.

Ogoh, S., Hayashi, N., Inagaki, M., Ainslie, P. N., & Miyamoto, T. (2008). Interaction between the ventilatory and cerebrovascular responses to hypo- and hypercapnia at rest and during exercise. *The Journal of Physiology*, *586*, 4327–4338.

Palecek, F. (1969). Measurement of ventilatory mechanics in the rat. *Journal of Applied Physiology*, *27*, 149–156.

Weil, J. V., Byrne-Quinn, E., Sodal, I. E., Kline, J. S., McCullough, R. E., & Filley, G. F. (1972). Augmentation of chemosensitivity during mild exercise in normal man. *Journal of Applied Physiology*, *33*, 813–819.

Smith, S. A., Mitchell, J. H., & Garry, M. G. (2006). The mammalian exercise pressor reflex in health and disease. *Experimental Physiology*, *91*, 89–102.

Strange, S., Secher, N. H., Pawelczyk, J. A., Karpakka, J., Christensen, N. J., Mitchell, J. H., & Saltin, B. (1993). Neural control of cardiovascular responses and of ventilation during dynamic exercise in man. *The Journal of Physiology*, *470*, 693–704.

Wasserman, K., Whipp, B. J., & Castagna, J. (1974). Cardiodynamic hyperpnea: Hyperpnea secondary to cardiac output increase. *Journal of Applied Physiology*, *36*, 457–464.

Wasserman, K., Whipp, B. J., & Casaburi, R. (1986). The respiratory system. control of breathing. In Cherniack, N. S. & Widdicombe, J. (Eds.), *Handbook of physiology*, section 3, *The respiratory system*, vol. *II, Control of breathing* (pp. 595–620). Bethesda: American Physiological Society.

Waldrop, T. G., Mullins, D. C., & Millhorn, D. E. (1986). Control of respiration by the hypothalamus and by feedback from contracting muscles in cats. *Respiration Physiology*, *64*, 317–328.

Whipp, B. J., & Pardy, R. L. (1986). Breathing during exercise. In Macklem, P. & Mead, J. (Eds.), *Handbook of physiology*, section 3, *The respiratory system*, vol. III, *Mechanics of breathing* (pp. 605–629). Bethesda, MD: American Physiological Society.

APPENDIX

The metabolic hyperbola has been described conventionally by:

$$P_{aCO_2} = 863 \times \dot{V}_{CO_2(STPD)}/\dot{V}_{A(BTPS)} \tag{1}$$

where $\dot{V}_A$ is alveolar ventilation, and 863 is a correction factor (Whipp & Pardy, 1986). This conventional metabolic hyperbola ignores the scaling factors representing ventilatory work-related CO_2 production.

We modified the conventional metabolic hyperbola as follows. If we approximate $\dot{V}_A$ by $\dot{V}_E \times (1 - V_D/V_T)$ and take into consideration the work of breathing (Aaron et al., 1992; Crosfill & Widdicombe, 1961; Harms et al., 2000), Equation (1) can be rewritten as

$$P_{aCO_2} = 863 \times (\alpha + \beta \times \dot{V}_E) / \left(\dot{V}_E \times \left[1 - V_D/V_T \right] \right) \tag{2}$$

where V_D/V_T represents dead space ventilation, and α and β are the respective scaling factors representing CO_2 production unrelated and related to work of breathing. Rearranging Equation (2) yields

$$P_{aCO_2} = A/\dot{V}_E + C \tag{3}$$

where $A = 863 \times \alpha/(1 - V_D/V_T)$ and $C = 863 \times \beta/(1 - V_D/V_T)$

Equation (3) is the modified metabolic hyperbola. The fitted parameters of A and C for the plant element (Equation (3)) take into account the metabolic changes incurred through ventilatory work-related CO_2 production as well as physiological dead space ventilation accompanying changes in respiration pattern and/or ventilation to perfusion ratio ($\dot{V}_A/\dot{Q}$). These changes are significant under specific environments and pathophysiological conditions.